Glycogen degrading activities of catalytic domains of α-amylase and α-amylase-pullulanase enzymes conserved in *Gardnerella* spp. from the vaginal microbiome

Pashupati Bhandari[1], Jeffrey Tingley[2], D. Wade Abbott[2] and Janet E. Hill[1,*]

[1]Department of Veterinary Microbiology, University of Saskatchewan, Saskatoon, Saskatchewan, Canada

[2]Lethbridge Research and Development Centre, Agriculture and Agri-Food Canada, Lethbridge, Alberta, Canada

*Correspondence: Janet.Hill@usask.ca

Abstract

Gardnerella spp. are associated with bacterial vaginosis, in which normally dominant lactobacilli are replaced with facultative and anaerobic bacteria including *Gardnerella* spp. Co-occurrence of multiple species of *Gardnerella* is common in the vagina and competition for nutrients such as glycogen likely contributes to the differential abundances of *Gardnerella* spp. Glycogen must be digested into smaller components for uptake; a process that depends on the combined action of enzymes collectively known as amylases. In this study, the ability of culture supernatants of 15 isolates of *Gardnerella* spp. to produce glucose, maltose, maltotriose and maltotetraose from glycogen was demonstrated. Carbohydrate active enzymes were identified bioinformatically in *Gardnerella* proteomes using dbCAN2. Identified proteins included a single domain α-amylase (encoded by all 15 isolates) and an α-amylase-pullulanase containing amylase, carbohydrate binding modules and pullulanase domains (14/15 isolates). To verify the sequence-based functional predictions, the amylase and pullulanase domains of the α-amylase-pullulanase, and the single domain α-amylase were each produced in *E. coli*. The α-amylase domain from the α-amylase-pullulanase released maltose, maltotriose and maltotetraose from glycogen, and the pullulanase domain released maltotriose from pullulan, demonstrating that the *Gardnerella* α-amylase-pullulanase is capable of hydrolyzing α-1,4 and α-1,6 glycosidic bonds. Similarly, the single domain α-amylase protein also produced maltose, maltotriose and maltotetraose from glycogen. Our findings show that *Gardnerella* spp. produce extracellular amylase enzymes as 'public goods' that can digest glycogen into maltose, maltotriose and maltotetraose that can be used by the vaginal microbiota.

Importance

Increased abundance of *Gardnerella* spp. is a diagnostic characteristic of bacterial vaginosis, an imbalance in the human vaginal microbiome associated with troubling symptoms, and negative reproductive health outcomes, including increased transmission of sexually transmitted infections and preterm birth. Competition for nutrients is likely an important factor in causing dramatic shifts in the vaginal microbial community but little is known about the contribution of bacterial enzymes to the metabolism of glycogen, a major food source available to vaginal bacteria. The significance of our research is characterizing the activity of enzymes conserved in *Gardnerella* species that contribute to the ability of these bacteria to utilize glycogen.

Introduction

Gardnerella spp. are associated with bacterial vaginosis (BV), a condition characterized by the replacement of the usually dominant *Lactobacillus* community with a mixture of facultative and anaerobic bacteria including *Gardnerella* spp. (1). BV is characterized by thin, white to greyish discharge and unpleased 'fishy' vaginal odor, however a large majority of women diagnosed with BV do not have symptoms (2). Phenotypic diversity among *Gardnerella* spp. may explain why they are found in women presenting clinical signs of bacterial vaginosis and in asymptomatic or BV negative women (3). The genus *Gardnerella* has been classified into four different species and at least 13 "genome species" (4). Co-occurrence of multiple *Gardnerella* species in the vaginal environment is common, and different species are dominant in different women (5). Given the potentially different roles of *Gardnerella* species in the vaginal microbiome, understanding the factors contributing to their population structure is important. Previous work has shown that interactions in co-cultures of *Gardnerella* spp. are typical of a "scramble"

59 competition (6), suggesting that competition for nutrients is an important factor contributing to the
60 differential abundances of *Gardnerella* spp. in the vaginal microbiome.

61 Glycogen is an abundant carbon and energy source available to the vaginal microbiota
62 including *Gardnerella*. Glycogen is a glucose homopolysaccharide comprising linear α-1,4 linked
63 glucose with α-1,6 branch points occurring approximately at every 8-13 residues to from a highly
64 branched and complex structure. The sizes of glycogen molecules and branching patterns can vary
65 based on the glycogen source (7). In the vagina, glycogen accumulates inside vaginal epithelial
66 cells under the influence of estrogen (8) and is released into the vaginal lumen through the activity
67 of bacterial cytolysins and/or lactic acid mediated acidosis (9). The amount of free glycogen in
68 vaginal fluid can range from undetectable to 32 μg/ml (10).

69 Glycogen must be digested into smaller products for uptake into bacterial cells. This
70 complex and multistep process requires the combined action of enzymes collectively known as
71 amylases. The majority of Glycogen degrading bacterial amylases belong to the glycosyl hydrolase
72 (GH) class within family 13 in the classification of carbohydrate active enzymes. GH13 enzymes
73 are further classified into more than 40 subfamilies based on their structure and substrate
74 specificity (11). Previous studies have shown the presence and activity of human and/or bacterial
75 amylases in vaginal fluid (12, 13) but the specific contribution of *Gardnerella* spp. to glycogen
76 digestion is not clear.

77 This study aimed to assess the glycogen digestion ability of *Gardnerella* spp. isolated from
78 the vaginal microbiome and to determine the distribution of extracellular glycogen degrading
79 enzymes among different species. In addition, we aimed to biochemically characterize the
80 activities of the predicted functional domains of extracellular glycogen degrading amylase

81 enzymes identified. Our findings showed that *Gardnerella* spp. have α-amylase and α-amylase-
82 pullulanase enzymes which can digest glycogen into maltose and other oligosaccharides.
83
84 **Methods**
85 ***Gardnerella* isolates**
86 Isolates of *Gardnerella* used in this study were from a previously described culture
87 collection (14) and included a total of 15 *Gardnerella* spp. isolates [three representative strains
88 each from *G. leopoldii* (GH005, VN003 & NR017), *G. piotii* (VN002, GH007 & GH020), *G.*
89 *vaginalis* (NR038, NR001 & NR039) and *G. swidsinskii* (NR016, NR021 & NR020), two isolates
90 from *Gardnerella* genome sp. 3 (NR026 & N170) and one from unknown genome species (NR047,
91 subgroup D based on cpn60 classification system). Whole genome sequence data for all isolates
92 were retrieved from NCBI BioProject Accession PRJNA394757.
93 **Amylase activity assay**
94 Amylase activity of *Gardnerella* isolates was assessed using a glycogen iodine test (15).
95 Isolates were revived from -80°C storage on Columbia blood agar plates containing 5% sheep
96 blood, and incubated anaerobically using the GasPak system (BD, USA) at 37°C for 48 hours.
97 Isolated colonies were transferred into modified NYCIII broth (obtained by replacing horse serum
98 with bovine serum and omitting glucose in NYCIII media) and incubated anaerobically for 24
99 hours at 37°C. Overnight broth cultures were centrifuged at 10,000 × *g* for 10 mins and the cell-
100 free supernatant was passed through a 0.45 µm filter. Filtered supernatant (10 µL) was spotted on
101 to a 1% (w/v) glycogen (Bovine liver glycogen, Sigma) agar plate and incubated anaerobically at
102 37°C for 24 hours. Filtered supernatant was also streaked on Columbia sheep blood agar to confirm
103 sterility. Plates were flooded with 1% (w/v) Lugol's iodine solution to detect evidence of amylase

104 activity. α-amylase from *Bacillus licheniformis* (0.05 mg/ml) (Sigma-Aldrich, Oakville, ON, CAT
105 No. A455) and modified NYCIII broth were used as positive and negative controls respectively.

106 **Activity of cell culture supernatants on glycogen**

107 Activity of cell culture supernatants on glycogen was assessed by incubating culture
108 supernatants with glycogen and examining the products. Briefly, 20 µl of culture supernatant was
109 added to 180 µl of 0.1% bovine liver glycogen in 50 mM sodium phosphate buffer, pH 7.0 and
110 incubated at 37ºC. Aliquots (50 µl) of the reaction mixture were collected at 24 h and were frozen
111 immediately until analysis by thin layer chromatography (TLC) and high-performance anion
112 exchange chromatography with pulsed amperometric detection (HPAEC-PAD). TLC was
113 performed on silica plates in a 1-butanol, acetic acid and distilled water (2:1:1 [vol:vol:vol]) mobile
114 phase and stained using 0.3% of N-napthyl ethylenediamine dihydrochloaride (Sigma) as
115 described previously (16). HPAEC-PAD samples were first precipitated with 80% ethanol to
116 remove large polysaccharides and diluted (to 1:20 for G5 and maltodextrin or 1:10 for glycogen)
117 and resolved on a Dionex PA20 column in a mobile phase of 30 mM NaOH and gradient of 10
118 mM to 120 mM sodium acetate over 40 min at a flow rate of 0.5 ml min^{-1}. Data were analyzed
119 using Chromeleon v6.80 chromatography data system software.

120 **Identification of the carbohydrate active enzymes (CAZyme)**

121 The *Gardnerella* proteomes, predicted from the RAST annotation, were uploaded into the
122 dbCAN2 webserver (22). All three available domain prediction tools (HMMER, eCAMI and
123 DIAMOND) were used to annotate the carbohydrate active domain(s) in protein sequences. The
124 dbCAN2 uses SignalP to predict whether a signal peptide is present or absent in the protein in
125 which each carbohydrate active domain is located. To identify secreted glycogen degrading
126 glycosyl hydrolases, dbCAN2 output was filtered to include only GH13 domain(s) associated with

127 signal peptide. TMHMM 2.0 (23) and LocateP (24) were used to predict transmembrane and cell-
128 wall anchored domains respectively.

129 **Phylogenetic analysis of GH13_32 amylase domains**

130 Domains belonging to subfamily 32 within the family 13 of glycosyl hydrolases class are
131 referred to as GH13_32 amylase domains. Amino acid sequences corresponding to the GH13_32
132 amylase domain were extracted from predicted extracellular glycosyl hydrolases of all study
133 isolates and four *Gardnerella* reference strains [(*G. leopoldii*, (CP029984)), *G. piotii*
134 (QJUV00000000), *G. vaginalis* (QJUZ00000000) and *G. swidsinskii* (QJVB00000000)](4).
135 Multiple-sequence alignments were performed using CLUSTALw and a neighbour joining
136 consensus tree was built in Geneious prime version 2022.1.1 (https://www.geneious.com). The
137 final tree was visualized using Figtree (v1.4.4).

138 To identify the conserved catalytic residues in GH13_32 domains, amino acid sequences
139 of representative GH13_32 domains of *G. leopoldii* NR017 were combined with GH13_32 domain
140 sequences from functionally characterized α-amylases [*Pseudoalteromonas haloplanktis* A23
141 (CAA41481.1) and *Streptomyces venezuelae* ATCC 15068 (AAB36561.1)] and amylopullulanase
142 [*Bifidobacterium breve* UCC2003 (AAY89038.1)] deposited in the CAZy database. Sequences
143 were aligned using CLUSTALw and alignments were visualized in ESPript (25).

144 **Expression and purification of α-amylase and pullulanase domains from α-amylase-**
145 **pullulanase**

146 To characterize activities of the amylase and pullulanase domains of the α-amylase-
147 pullulanase, *G. leopoldii* (NR017) was chosen as a representative isolate. Genomic DNA was
148 extracted from *G. leopoldii* NR017 using a modified salting out procedure. Primers
149 (Supplementary Table 1) were designed to amplify the nucleotide sequences encoding the

150 predicted α-amylase (corresponding to amino acids 74-350 of Genbank Accession RFT33565) and
151 pullulanase (corresponding to amino acids 1141-1462 of Genbank Accession RFT33565) domains
152 of the NR017 α-amylase-pullulanase gene along with 30 additional flanking nucleotides each on
153 the 5' and 3' ends. PCR was carried out in PCR buffer (0.2 M Tris-HCl [pH 8.4], 0.5 M KCl), a
154 200 mM concentration of each deoxynucleoside triphosphate (dNTP), 2.5 mM $MgCl_2$, a 400 nM
155 concentration of each primer (α-amylase: JH0810-F & JH0811-R, or pullulanase: JH0812-F &
156 JH0813-R), 1 U/reaction of Platinum Taq DNA polymerase high-fidelity (5 U/ml in 50% glycerol,
157 20 mM Tris-HCl, 40 mM NaCl, 0.1 mM EDTA, and stabilizers) (Life Technologies), and 2 μl of
158 template DNA, in a final volume of 50 μl. PCR was performed with the following parameters:
159 initial denaturation at 94°C for 3 min, 40 cycles of denaturation at 94°C for 15 s, annealing at 60°C
160 for 15 s, and extension at 72°C for 1 min (for α-amylase domain) or 1.5 min (for pullulanase
161 domain), and final extension at 72°C for 3 min. Purified PCR products were digested with *Bam*HI
162 and *Kpn*I and ligated into expression vector pQE-80L treated with the same restriction
163 endonucleases. The pQE-80L+amylase domain plasmid (henceforth referred to as pQE80L-AMY)
164 was used to transform chemically competent *E. coli* Rosetta DE3 cells (Novagen, Sigma-Aldrich),
165 and the pQE-80L+pullulanase domain plasmid (henceforth referred to as pQE80L-PULL) was
166 used to transform One Shot TOP10 chemically competent *E. coli* cells (Invitrogen, Carlsbad, CA).
167 Insertion of amylase and pullulanase domain encoding sequences in frame with the N-terminal
168 His-tag was confirmed by sequencing of the purified plasmid.

169 *E. coli* Rosetta cells containing pQE80L-AMY were grown in 800 ml of LB broth
170 containing ampicillin (100 μg/ml) and chloramphenicol (25 μg/ml) whereas *E. coli* Top10 cells
171 containing pQE80L-PULL were grown in same volume of LB broth with ampicillin (100 μg/ml)
172 only. Once the culture reached an optical density at 600 nm (OD_{600}) of 0.4 - 0.6, protein expression

173 was induced with 0.5 mM IPTG. After 4 h of incubation at 37°C with shaking at 200 rpm, cells
174 were harvested by centrifugation at 8500 × *g* for 20 min at 4°C and pellets were stored at -20°C
175 until further processing. Proteins were solubilized using anionic detergent as described previously
176 (26) with a slight modification during sonication (6 min total run time, 2 min on, 1 min off at 4°C).
177 Eluted proteins were dialyzed against 1 × PBS (pH 7.4) at 4°C using a semipermeable membrane
178 with cut-off size 12 kDa for 24 - 48 hours. The diluted proteins were concentrated using a 30 kDa
179 molecular weight cut-off protein concentrator (Thermo Fisher Scientific). Final protein
180 concentration was measured using a Nanodrop spectrophotometer before storing at -20°C.

181 **Expression and purification of single amylase domain containing α-amylase**

182 A codon-optimized DNA construct corresponding to the full-length open reading frame of
183 single domain α-amylase from *G. leopoldii* NR017 was synthesized and a region encoding amino
184 acids 58-519 (excluding N-terminal signal peptide and C-terminal transmembrane domain) was
185 amplified using JH0857 and JH0858 primers (Supplementary Table 1). The 1463 bp product was
186 ligated into *Mfe*I *and Hind*III digested pET41a+ vector to express as a N-terminal GST-His tag
187 fusion protein (79.9 kDa). The recombinant plasmid (pET41a+CO-AMY) was used to transform
188 chemically competent *E. coli* DH5α cells. Presence of the insert in frame with the N-terminal
189 GST-His-tag was confirmed by Sanger sequencing of the purified plasmid.

190 Purified recombinant plasmid (pET41a+CO-AMY) was used to transform *E. coli*
191 BL21DE3 cells for protein production. *E. coli* BL21DE3 cells containing recombinant plasmid
192 were grown in 1.8 L of LB broth containing kanamycin (30 μg/ml). When culture reached to
193 optical density OD_{600} 0.4 - 0.6, IPTG was added to a final concentration of 0.5 mM to induce
194 protein expression at 37ºC for 4 hours with shaking at 200 rpm. Cells were harvested by
195 centrifugation at 8500 × *g* for 20 min. Expressed protein was solubilized using anionic detergent

196 as described previously (26) with slight modification of the sonication protocol (80% duty cycle,
197 8 minutes total run time, 10 secs on, 5 secs off). The recombinant amylase protein was purified
198 using a nickel column. Eluted proteins were dialyzed against 1× PBS (pH 7.4) at 4°C overnight
199 using a semipermeable membrane of cut-off size 12 kDa, and dialyzed protein was concentrated
200 using a 30 kDa molecular weight cut-off protein concentrator (Thermo Fisher Scientific). Final
201 protein concentration was measured using a Nanodrop spectrophotometer before storing at -20°C.
202 The region encoding the GST and 6xHis tags was expressed from empty pET41a vector in
203 *E. coli* BL21DE3 cells and was purified using Ni-affinity chromatography for use as a negative
204 control in activity experiments.

205 **Enzyme activity on different substrates**

206 The activity of purified enzymes was tested by incubating purified enzymes with different
207 substrates. Briefly, 250 µl of the purified amylase domain (22.3 µM) or α-amylase (13.0 µM) was
208 incubated with 1% glycogen, maltodextrin (dextrose equivalent 13-17) or maltopentose while
209 purified pullulanase (25.3 µM) was incubated with 1% pullulan. All substrates were prepared in
210 50 mM sodium phosphate buffer at pH 6.0. Enzyme substrate reaction mixtures were incubated at
211 37ºC for 24 h and stored at -20°C until further analysis by TLC or HPAEC-PAD as described
212 above.

213

214 **Results**

215 **Amylase activity of *Gardnerella* culture supernatants**

216 No growth was observed from filtered culture supernatants, confirming their sterility.
217 Supernatants of all 15 isolates showed amylase activity in the agar plate assay (Figure 1). Cell-free
218 culture supernatants of 14 isolates produced glucose, maltose, maltotriose from glycogen while

219 glucose was the only product detected from N170 supernatant (*Gardnerella* genome sp. 3, GS3-

220 2) (Figure 2).

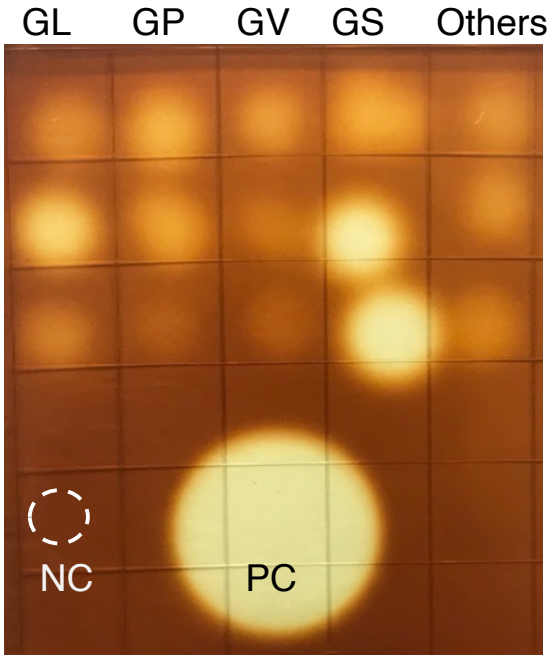

221

222 Figure 1: Amylase activity of cell free culture supernatants on glycogen agar. Each spot represents
223 one isolate and a total of 15 different isolates, three each from GL: *G. leopoldii*, GP: *G. piotii*,
224 GV: *G. vaginalis*, GS: *G. swidsinskii* and others [two isolates from *Gardnerella* genome sp. 3 (top
225 & middle) and one isolate from unknown genome species (bottom) (corresponds to the subgroup
226 D based on cpn60 classification system)] are shown. NC: mNYC, PC: *B. licheniformis* amylase
227 (0.05 mg/ml).
228

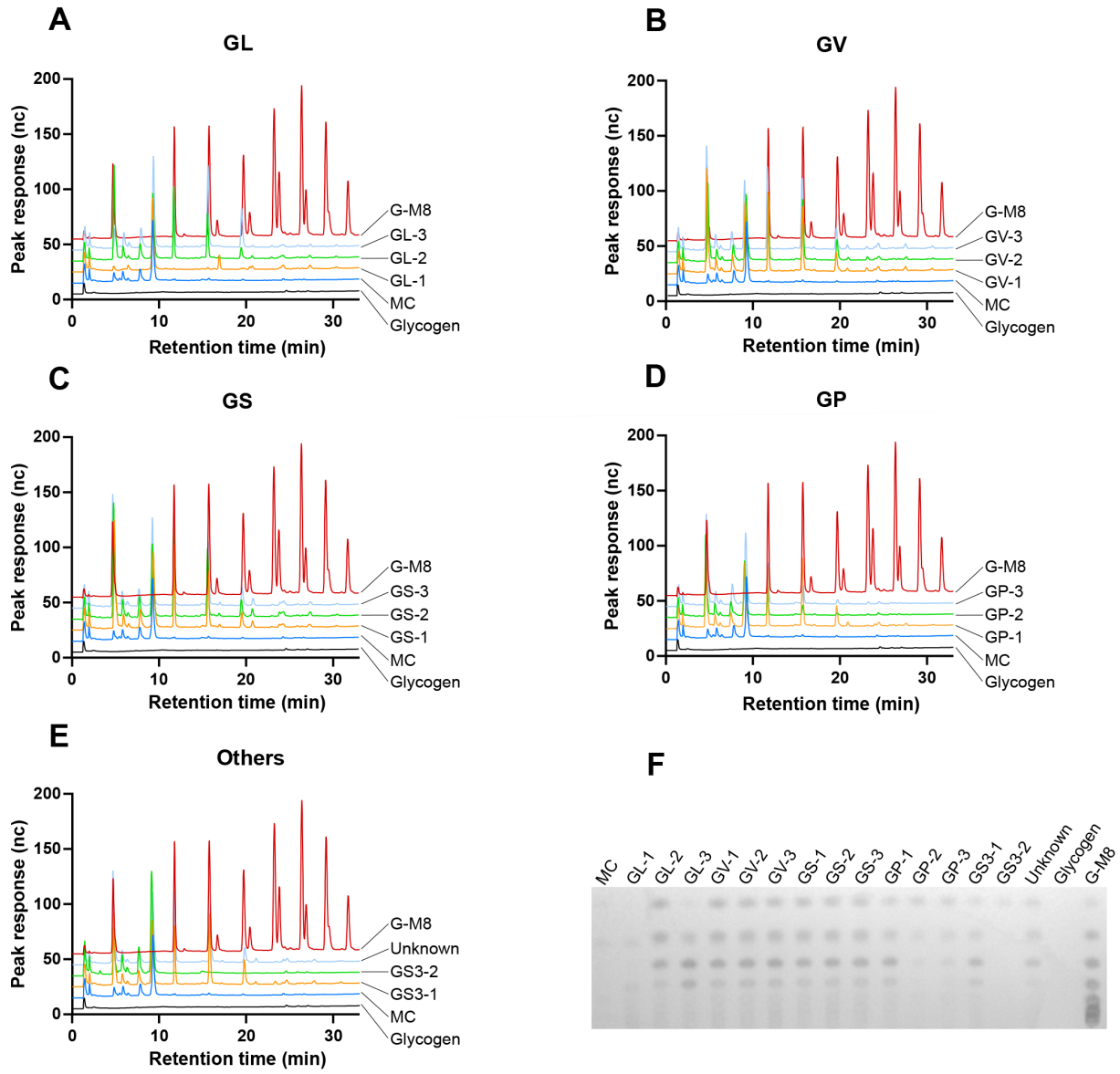

Figure 2: Identification of glycogen breakdown products produced after 24 h by culture supernatants of 15 *Gardnerella* isolates by HPAEC-PAD (A-E) and TLC (F). GL: *G. leopoldii*, GV: *G. vaginalis*, GS: *G. swidsinskii*, GP, *G. piotii*, and others [two isolates from *Gardnerella* genome sp. 3 (top & middle) and one isolate from unknown genome species (bottom) (corresponds to the subgroup D based on cpn60 classification system)], MC: media control, G-M8: glucose to maltooctaose standards.

238 **Identification of genes encoding carbohydrate active enzymes in *Gardnerella* genomes**

239 Out of 20,017 predicted protein sequences from 15 isolates uploaded into the dbCAN2
240 webserver, 886 sequences had at least one carbohydrate active domain. Results were filtered to
241 include only glycosyl hydrolase (GH) domains associated with a signal peptide. Only 52/836
242 sequences identified as belonging to the GH class had an associated signal peptide. Results were
243 further filtered to identify predicted extracellular glycogen degrading enzymes (protein containing
244 at least one GH13 domain associated with signal peptide), resulting in identification of 29
245 sequences.

246 A multidomain enzyme containing an N-terminal α-amylase domain (GH13_32), followed
247 by 2 - 4 carbohydrate binding modules (CBM, of types CBM25, CBM41 or CBM48) and a C-
248 terminal pullulanase domain (GH13_14) was identified in all isolates except N170. This enzyme
249 also included an N-terminal signal peptide domain, C-terminal transmembrane domain and a cell
250 wall anchor LPxTG domain (Figure 3A). This multidomain enzyme is traditionally referred to as
251 Type II amylopullulanase, however, recently it has been suggested that these enzymes are more
252 appropriately classified as Type II α-amylase-pullulanase (27) and so the term 'α-amylase-
253 pullulanase' is used throughout this paper. The domain organization of *G. leopoldii* NR017 α-
254 amylase-pullulanase (RFT33565.1) is shown in Figure 3A. Similarly, a single α-amylase
255 (GH13_32) domain containing α-amylase enzyme with an N-terminal signal peptide and a C-
256 terminal transmembrane domain was identified in all 15 isolates (NR017 accession number
257 RFT33564.1) (Figure 3B).

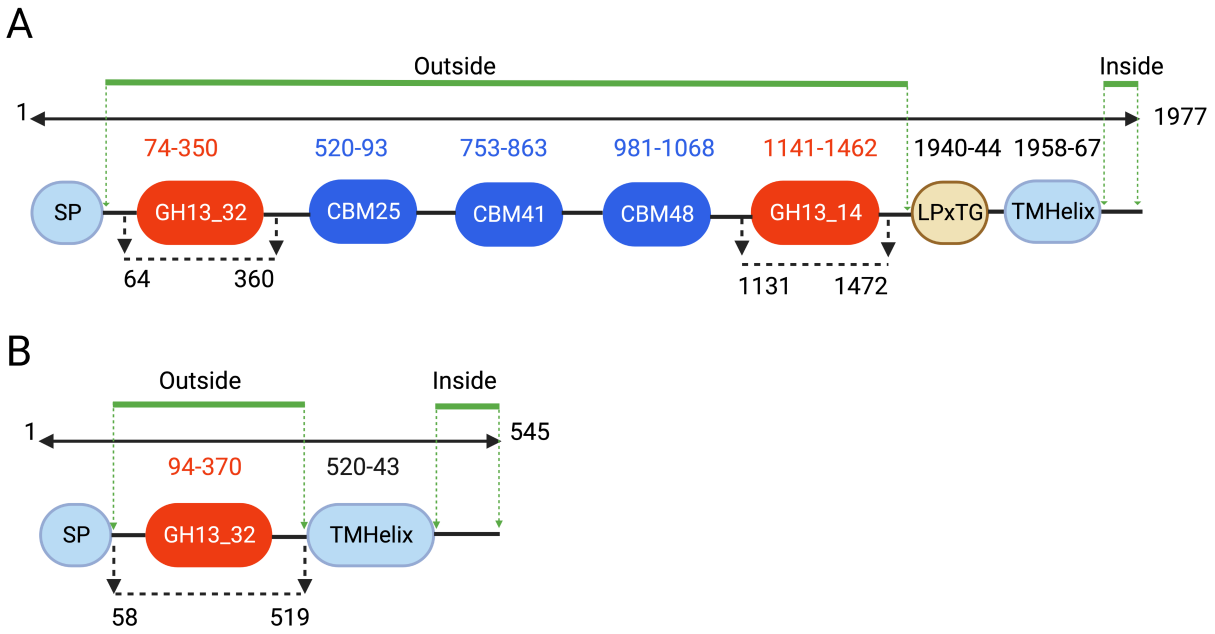

Figure 3: Predicted domains of *G. leopoldii* NR017 α-amylase-pullulanase (1977 amino acids) (A) and α-amylase (545 amino acids) (B). Amylase and pullulanase domains belonging to GH13 subfamilies 32 and 14 are indicated in red while three carbohydrate binding modules (CBM) are in blue. SP, Signal peptide; LPxTG, Cell-wall anchoring LPxTG domain, TMHelix, transmembrane helix domain respectively. Numbering indicates amino acid positions. The regions used for recombinant protein expression are indicated with black broken line with arrows. Predicted extracellular and intracellular regions are indicated with green lines.

Phylogenetic analysis of GH13_32 amylase domains and relationship with other amylases

GH13_32 amylase domain sequences from the single domain α-amylase and α-amylase-pullulanase from all study isolates formed two distinct clusters (Figure 4A). Intra-cluster amino acid sequence identity of amylase domains within single domain α-amylase and α-amylase-pullulanase enzymes was 75-100% and 66-100%, respectively, whereas inter-cluster identity was 64-74%.

GH13 enzymes have a conserved catalytic triad of two aspartate residues (acts as a nucleophile and to stabilize the transition state) and a glutamate residue (general acid base) (28). *In silico* analysis of GH13_32 amylase domains of *G. leopoldii* NR017 with GH13_32 amylase domains of functionally characterized α-amylase and α-amylase-pullulanase revealed conserved

catalytic residues (Figure 4B). The catalytic triad was conserved across all GH13_32 amylase domains from 15 *Gardnerella* isolates. (Supplementary Figure 1).

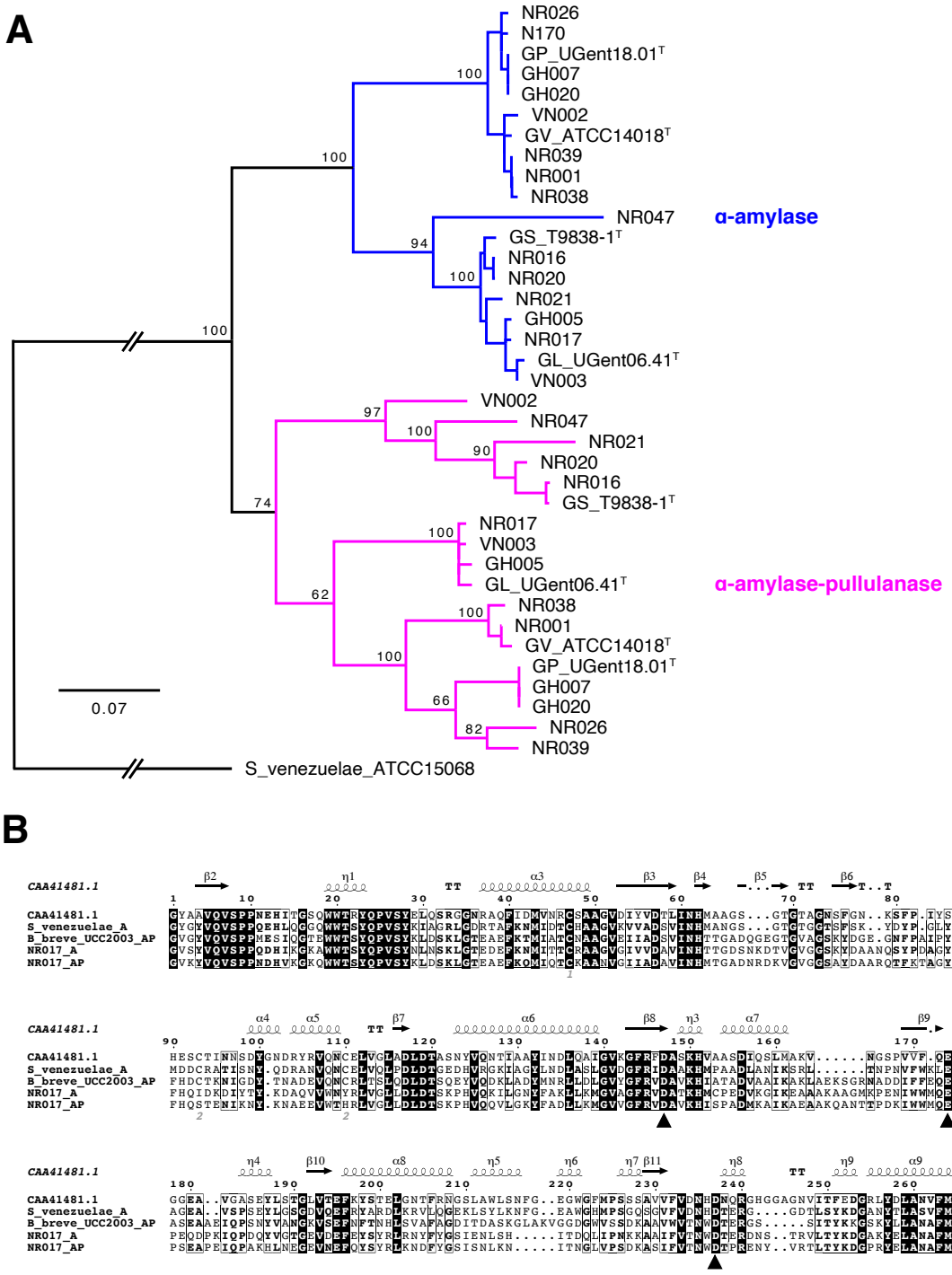

Figure 4: (A) Phylogenetic tree of all α-amylase domains from 15 *Gardnerella* isolates and 4 reference strains (indicated with T after the strain name). The tree is rooted with *Streptomyces venezuelae* ATCC15068. Trees are consensus trees of 100 bootstrap iterations and constructed

283 using Neighbour joining method using Tamura-Nei distance model. The number at major branch
284 points represents the percentage bootstrap support. (B) Sequence alignment of GH13_32 catalytic
285 domains of *G leopoldii* NR017 α-amylase (NR017_A) and α-amylase-pullulanase (NR017_AP)
286 with other functionally characterized GH13_32 members ((α-amylases from *Psuedoalternomonas*
287 *haloplanktis* A23 (CAA41481.4) and *S. venezuelae* ATCC15068) and 'amylopullulanase' from
288 *Bifidobacterium breve* UCC2003). Black triangles indicate conserved catalytic residues.

289

290 **Protein expression and purification**

291 The entire open reading frame of *G. leopoldii* NR017 α-amylase-pullulanase (GH13_32
292 and GH13_14) comprises 5,933 bp encoding a 1,977 amino acid protein with a predicted mass of
293 215.3 kDa (Figure 3A). The gene segments encoding the α-amylase (amino acids 64-360) and
294 pullulanase domains (amino acids 1131-1472) were each PCR amplified and ligated into pQE-
295 80L vector to express as N-terminal 6His-tagged proteins in *E. coli* (Figure 5A, left panel).
296 Expressed proteins were solubilized using 1% SDS and purified using nickel-nitriloacetic acid
297 (Ni-NTA) columns (Supplementary Figure 2). Apparent molecular weights of the 6His-tagged
298 amylase and pullulanase domains were 35.7 and 40.5 kDa, respectively (Figure 5B, left and
299 middle).

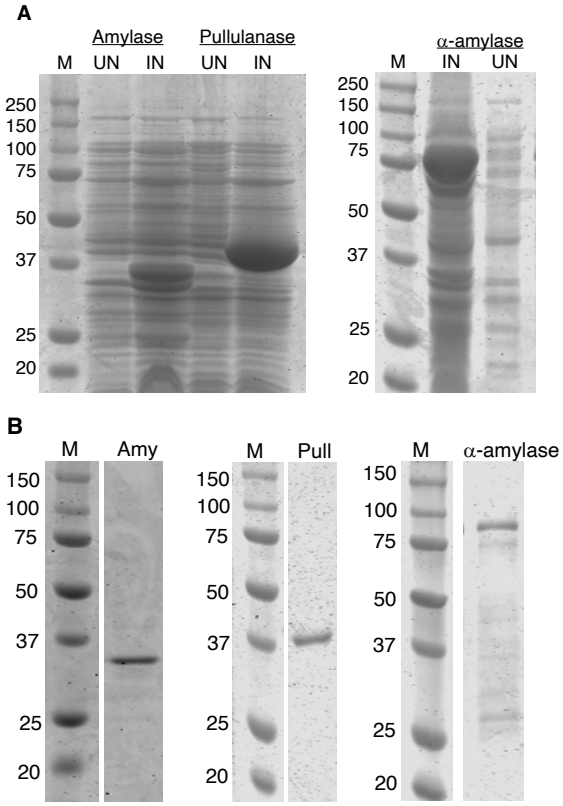

Figure 5: (A) Protein profiles of uninduced (UN) and induced (IN) *E. coli* cells containing pQE80L-AMY & pQE80L-PULL (top left) and pET41a+CO-AMY (top right) recombinant plasmids. (B) Purified 6His-tagged amylase (Amy) (bottom left) and pullulanase (Pull) (bottom middle) and GST-6His-tag α-amylase (bottom right). M molecular weight markers.

The *G. leopoldii* NR017 α-amylase enzyme (1635 bp encoding a 545 amino acid protein with a predicted mass of 60.5 kDa) has a predicted N-terminal signal peptide (amino acids 1-57) and C-terminal transmembrane domain (amino acids 520-545) (Figure 3B). A codon-optimized version of the truncated α-amylase gene sequence encoding amino acids 58-519 was expressed as a GST fusion protein with an apparent molecular weight of 79.9 kDa in *E. coli* BL21 DE3 cells (Figure 5A, right). The recombinant protein was solubilized using 1% SDS. Attempts to purify this GST fusion protein using glutathione beads resulted in a very low recovery of target protein due to poor binding to the beads (Supplementary Figure 3). The pET41a+amylase construct

314 includes an N-terminal hexa-histidine tag between the GST tag and the amylase sequence.
315 Purification of the fusion protein using a Ni-NTA column resulted in partial protein purification
316 (Figure 5B, right). Additional lower molecular weight peptides observed in the column eluate were
317 identified as degraded peptide fragments of the fusion protein by western blot with anti-His
318 antibodies (Supplementary Figure 4).

319 **Activity of the purified proteins**

320 The α-amylase domain from the α-amylase-pullulanase released maltose and maltotriose
321 from maltopentose while maltose, maltotriose and maltotetraose were identified as the major
322 products from maltodextrin (13-17) and glycogen (Figure 6A). The pullulanase domain produced
323 maltotriose as the only product from pullulan (Figure 6B). A small peak corresponding to
324 isomaltose was observed in the HPAEC-PAD results from 24 and 48 h digests of glycogen with
325 amylase domain (Figure 6A- middle right). Overall, our results show that amylase and pullulanase
326 domains from α-amylase-pullulanase can hydrolyse α-1,4 and α-1,6 glycosidic bonds,
327 respectively.

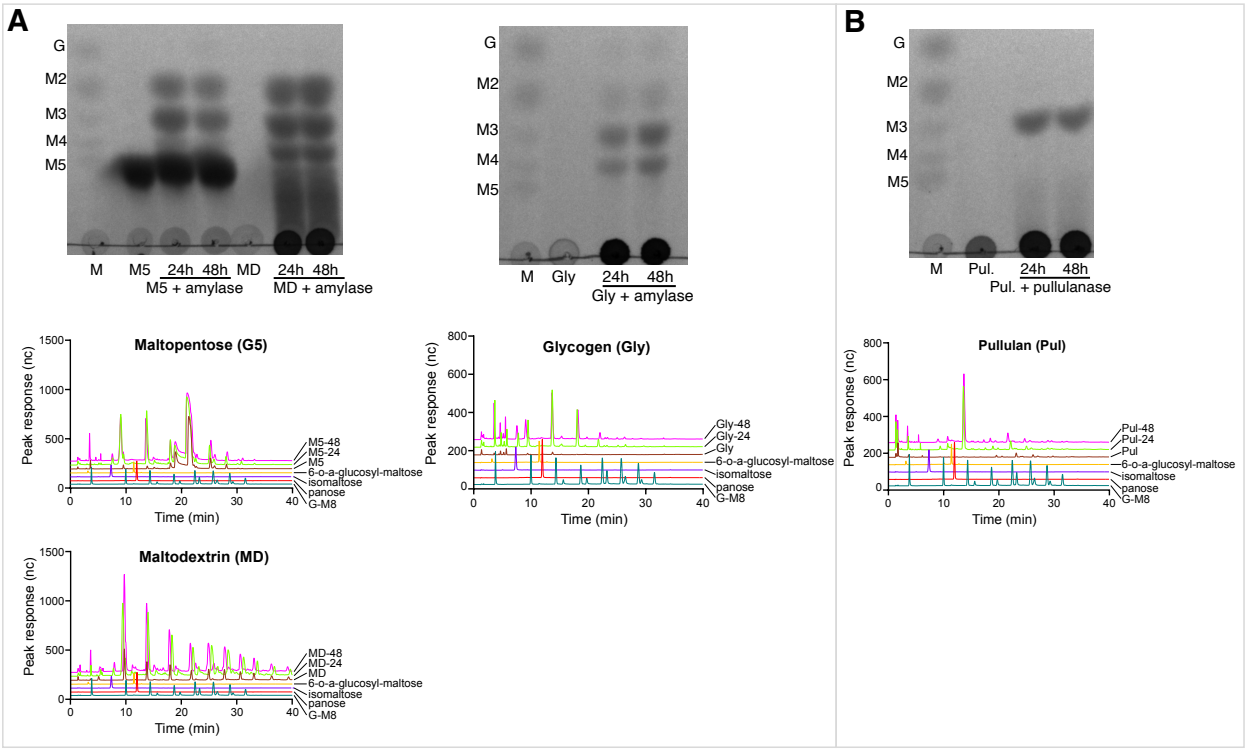

Figure 6: (A) Identification of products released by α-amylase domain (GH13_32) of α-amylase-pullulanase from maltopentose (M5) and maltodextrin (MD) and glycogen (Gly) after 24 and 48h of incubation using TLC (top) and HPAEC-PAD (middle and bottom). (B) Products released from pullulan by the pullulanase domain (GH13_14) after 24 and 48 h incubation were identified using TLC (top) and HPAEC-PAD (bottom). Standards in Lane M of each panel: G: glucose, M2: maltose, M3: maltotriose, M4: maltotetraose and M5: maltopentose.

Since the α-amylase domain from the single-domain α-amylase enzyme was expressed as a GST-6xHis fusion, we initially confirmed that no amylase activity was detected from the GST-6xHis tag (Supplementary Figure 5). Maltose and maltotriose were produced when maltopentose was incubated with single domain α-amylase (Figure 7A, top and middle). Similarly, maltose, maltotriose and maltotetraose were identified as the major products in the reaction mixture of glycogen with single domain α-amylase (Figure 7B). As expected, the maltodextrin substrate included maltose, maltotriose and maltotetraose, however, an increase in intensity of maltose, maltotriose and maltotetraose spots was observed in TLC results in the reaction mixture of single

344 domain α-amylase with maltodextrin when compared to a substrate only control (Figure 7A, top).

345 HPAEC-PAD analysis of products from maltodextrin also showed larger peaks of maltose,

346 maltotriose and maltotetraose relative to the control (Figure 7A, bottom).

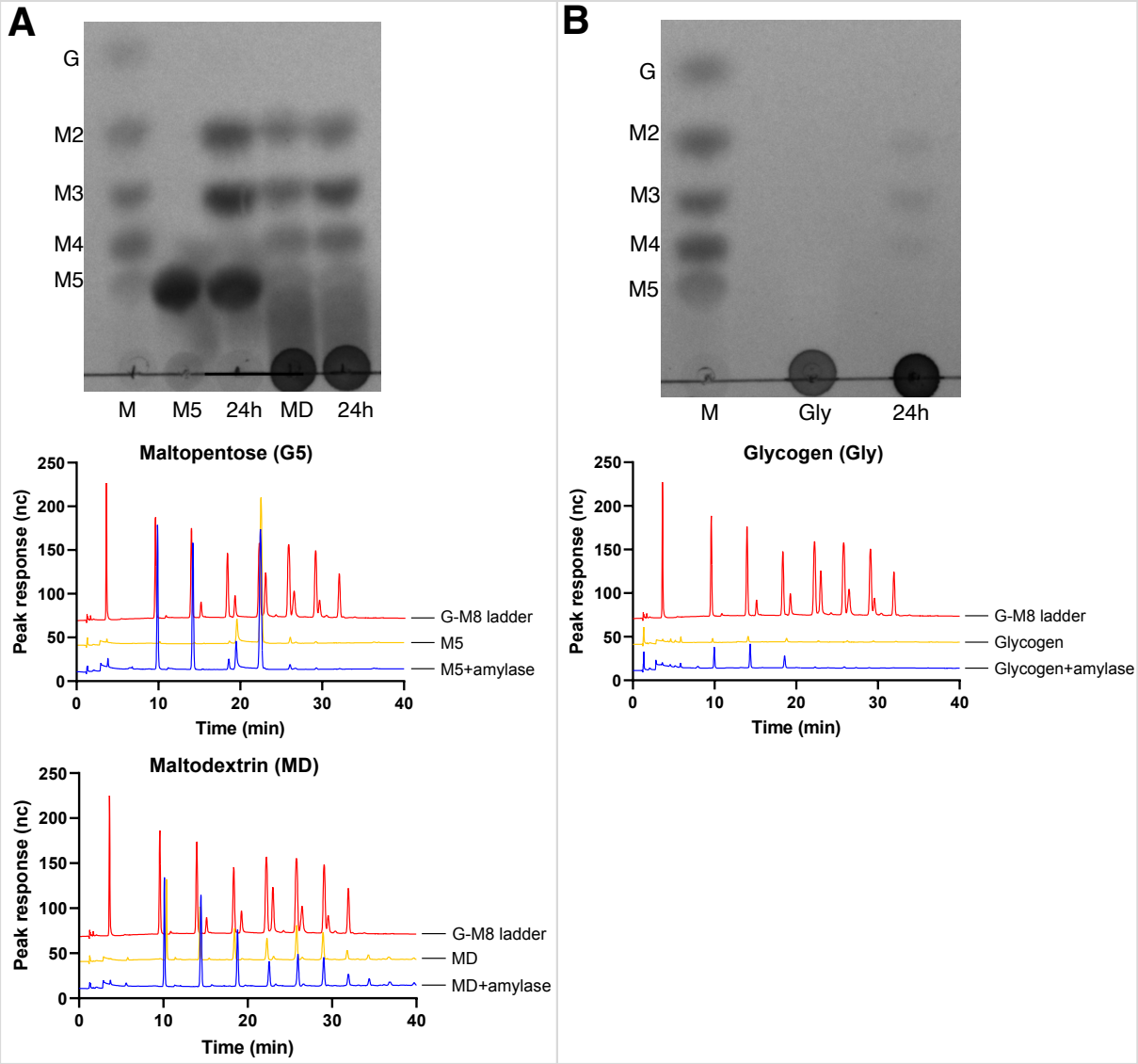

347

348 Figure 7: (A) Identification of products released by the purified single domain α-amylase enzyme
349 from maltopentose (M5) and maltodextrin (MD) using TLC (top) and HPAEC-PAD (bottom) after
350 24h incubation. (B) Products released from glycogen by the purified single domain α-amylase
351 enzyme after 24 h incubation were identified using TLC (top) and HPAEC-PAD (bottom).
352 Standards in Lane M of each panel: G: glucose, M2: maltose, M3: maltotriose, M4: maltotetraose
353 and M5: maltopentose.
354

355 **Discussion**

356 Dysbiosis in the vaginal microbiome has significant consequences that can affect the
357 quality of life and reproductive health of women. There are several hypotheses about how
358 dysbiosis is initiated and maintained (29, 30) but the ecological factors determining microbial
359 population dynamics in the vaginal microbiome are not well understood. In addition to direct
360 antagonistic (31) or synergistic (32) interactions among microbiota, changes in environmental
361 conditions due to pregnancy status, hormone levels, infection, sexual behaviour and hygiene
362 practices certainly play a role in determining the fitness of vaginal microbiota and thus microbial
363 community composition. *Gardnerella* spp. have been implicated in the initial stages of transition
364 to bacterial vaginosis (30) and so factors affecting their fitness, including their interaction with
365 vaginal glycogen, are of particular interest.

366 Glycogen breakdown is a complex and multistep process that requires the action of several
367 enzymes collectively known as amylases. Vaginal secretions contain host derived pancreatic α-
368 amylase and α-glucosidases that can digest glycogen into smaller sugars (12). Until recently, the
369 contribution of bacterial amylases in this process was unclear. Recently, van der Veer *et al.* showed
370 that vaginal isolates of *Lactobacillus crispatus* are capable of growing in glycogen supplemented
371 medium and encode type I pullulanase in their genomes (33). This study further reported that
372 strains showing less efficient or no growth on glycogen have an N-terminal deletion mutation in
373 their putative type I pullulanase gene suggesting its role in extracellular glycogen digestion. Forney
374 *et al.* identified eight putative amylases from vaginal metagenomes of *Bifidobacterium vaginale*,
375 *B. lacrimalis*, *L. gasseri*, *L. crispatus, L. iners* and *L. jensenni* and further reported that multiple
376 microbial amylases are present in vaginal fluid (13). Similarly, Woolston *et al.* identified putative
377 glycogen degrading enzymes in genomes of vaginal bacteria including *Gardnerella* spp. and

378 biochemically characterized the glycogen degradation ability of six GH13 hydrolase enzymes
379 (34) identified in those species. Together these findings suggest that bacterial enzymes contribute
380 to the breakdown of vaginal glycogen.

381 The genus *Gardnerella* was a mono-specific genus until recently when it was classified
382 into four species and additional "genome species" that have not yet been named due to insufficient
383 evidence (4). The role of *Gardnerella* spp. in extracellular glycogen digestion and whether the
384 species in this genus differ in digesting glycogen is not clear. Although earlier studies reported that
385 *Gardnerella* isolates can utilize glycogen (35–37), it is not clear if all newly defined species are
386 capable of digesting extracellular glycogen. In this study, we used cell free culture supernatants
387 from genetically characterized isolates to test extracellular glycogen breakdown ability of different
388 *Gardnerella* spp.

389 Selection of an appropriate culture medium to make culture supernatants is a challenge. As
390 our main interest was to identify the sugars released from glycogen, differentiating the background
391 sugars that are already present in medium from those obtained from glycogen hydrolysis is crucial.
392 *Gardnerella* is typically cultured in BHI broth or NYCIII and both media contain glucose. In
393 addition, the complement inactivated horse serum (obtained by heat treatment at 56ºC for 20
394 minutes) added to NYCIII can itself digest glycogen. It is reported that heat treatment at 70ºC for
395 20 minutes inhibits the maltase and amylase activity of fetal bovine serum but not horse serum
396 (38). For this reason, in our experiments a modified NYCIII media supplemented with heat
397 inactivated (70ºC for 20 minutes) fetal bovine serum instead of horse serum and no added glucose
398 was used to prepare culture supernatants. Cell free culture supernatants of all isolates tested
399 showed amylase activity in a glycogen agar plate assay, suggesting that glycogen degradation is a
400 conserved property in the genus *Gardnerella*. Glucose, maltose, maltotriose and maltotetraose

401 were identified as the major products released from glycogen by culture supernatants of all
402 *Gardnerella* isolates except N170 isolate which produced only glucose. Consistent with this
403 observation α-amylase-pullulanase genes were detected in all isolates except N170. Overall, no
404 species-specific patterns of glycogen breakdown products were found in *Gardnerella* spp.

405 Of the two predicted extracellular glycosyl hydrolases identified by dbCAN2, the α-
406 amylase-pullulanase contained separate amylase and pullulanase catalytic domains; a
407 conformation historically referred to as Type II amylopullulanase (39). With the availability of
408 more sequence data, these enzymes are now classified as Type II α-amylase-pullulanase and they
409 differ from amylopullulanases which have only one catalytic domain capable of hydrolyzing both
410 α-1,4 and α-1,6 glycosidic bonds (27).

411 The amylase and pullulanase domains of the α-amylase-pullulanase flanked 2 - 4 CBMs.
412 CBMs appended to GH13 enzymes are important for binding to different α-glucans, such as
413 amylose, amylopectin, glycogen, pullulan and oligosaccharides derived from these
414 polysaccharides (40, 41). CBMs increase the concentration of substrate on the enzyme surface and
415 their removal can significantly reduce enzyme activity. It is reported that removal of CBMs
416 reduced the activity of *Eubacterium rectale* α-amylase on starch by ~40 fold compared to the
417 wildtype protein (42). Similarly, compared to a full-length enzyme, removal of CBM domains
418 reduced the activity of *B. adolescentis* P2P3 Type II pullulanase on glycogen (43). We did not
419 investigate the roles of the CBMs in the α-amylase-pullulanase characterized in this study since
420 our attempts to express full-length α-amylase-pullulanase were unsuccessful.

421 Recently, Wollston *et al.* (34) characterized a full length 'amylopullulanase' (2013 amino
422 acids) from a vaginal isolate of *G. vaginalis* and reported maltose and maltotriose as the major
423 products from glycogen. In this report, the authors described the enzyme as containing two 'α-

424 amylase domains' rather than amylase and pullulanase catalytic domains as we describe here. By
425 expressing the two catalytic domains separately we have demonstrated that they have distinct
426 activities, hydrolysing α-1,4, and α-1,6 bonds, respectively.

427 Both α-amylase and α-amylase-pullulanase enzymes are active against oligosaccharides
428 and glycogen. Although the overall sequence identity between the two amylase domains
429 characterized in this study was only 64-74%, predicted catalytic residues were perfectly conserved
430 (Figure 4B). Either domain would thus be capable of acting on the malto-oligosaccharides
431 produced by the debranching activity of the pullulanase domain to generate glucose, maltose, and
432 other small oligosaccharides. This type of functional redundancy where two enzymes have similar
433 biochemical activities is common in bacteria (44).

434 Although *Gardnerella* α-amylase and α-amylase-pullulanase are predicted to be
435 extracellular, both enzymes have C-terminal transmembrane helices followed by a short
436 intracellular domain. A cell wall anchoring LPxTG domain was also identified in the α-amylase-
437 pullulanase sequence, immediately N-terminal to the transmembrane helix (Figure 3A). The
438 presence of these features suggests that both enzymes are tethered to the cell wall. Cell wall
439 anchored proteins can be released into the extracellular environment during bacterial growth as a
440 by-product of cell wall turnover or cell death or proteolytic cleavage (45), which is consistent with
441 our detection of amylase activity in sterile culture supernatants. Some *Gardnerella* species also
442 produce cell wall anchored sialidases, NanH2 and NanH3, that are also released into the
443 supernatant after cell death or by proteolytic cleavage (46).

444 Although glucose was identified as one of the major products in glycogen digests of
445 *Gardnerella* culture supernatants, the purified α-amylase domain and single domain α-amylase
446 proteins did not produce glucose from glycogen. TLC and HPAEC-PAD analysis showed that

447 glucose was neither produced by the activity of culture media itself nor present in glycogen
448 substrate (Figure 2F& 2G). Another possibility is that the activity of a full-length α-amylase-
449 pullulanase protein on glycogen might generate different product profiles than the isolated
450 domains. A full-length type II pullulanase enzyme (containing two separate α-amylase and
451 pullulanase domains) from *Bifidobacterium adolescentis* P2P3 was reported to produce maltose
452 only from glycogen, while the purified amylase domain protein from the same enzyme produced
453 a mixture of glucose, maltose and maltotriose (43). Glucose may also be produced by the activity
454 of intracellular α-glucosidase on malto-oligosaccharides generated from glycogen hydrolysis that
455 are released by dead/lysed bacteria in the culture. We have previously shown that *Gardnerella* spp.
456 have conserved intracellular α-glucosidase that can release glucose from smaller oligosaccharides
457 (47).

458 Our findings show that all *Gardnerella* species produce extracellular α-amylase and α-
459 amylase-pullulanase enzymes that are 'public goods' in the vaginal microbiome, breaking down
460 glycogen to produce similar fingerprints of glycogen derived products and contributing to the
461 nutrient pool available to the vaginal microbiota (Figure 8). Determining if these *Gardnerella* spp.
462 differentially utilize and compete for these breakdown products will provide insights into whether
463 competition for malto-oligosaccharides plays a role in determining *Gardnerella* community
464 structure in the vaginal microbiome.

465

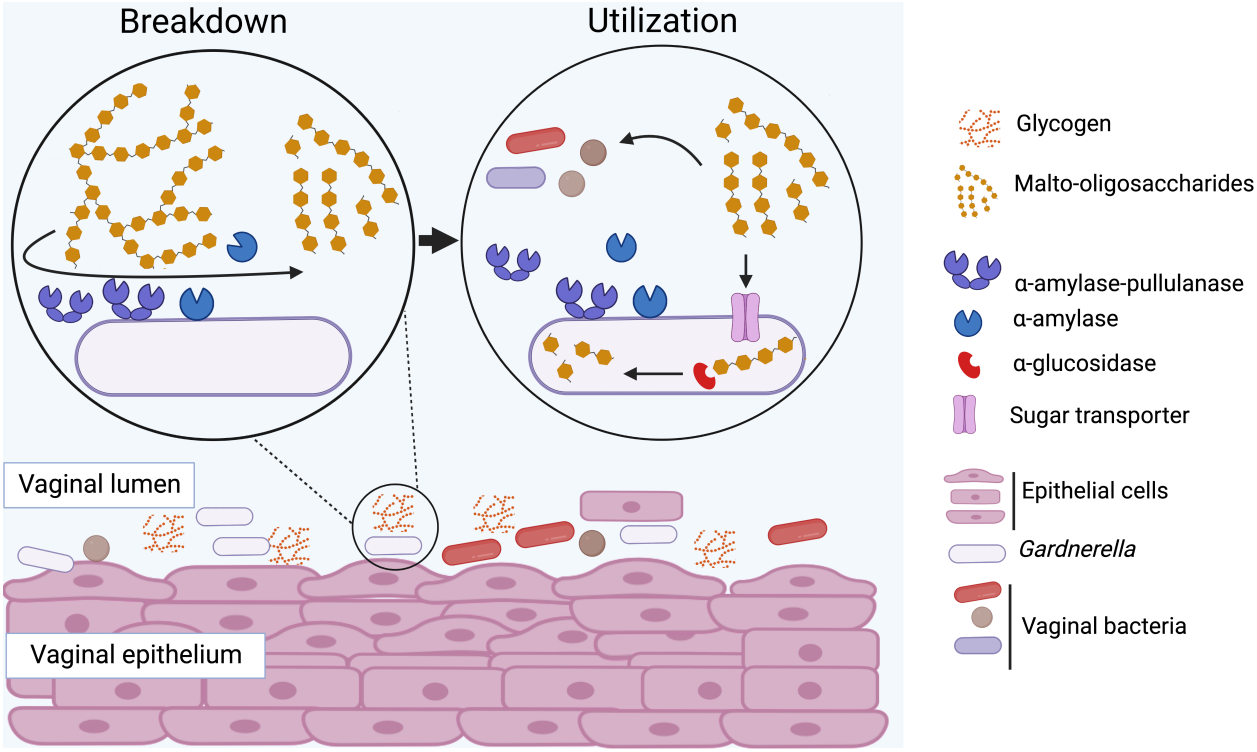

Figure 8: Proposed mechanisms of extracellular glycogen utilization in *Gardnerella* spp. Glycogen is digested into malto-oligosaccharides by α-amylase-pullulanase and α-amylase and these breakdown products are transported inside and can be further digested to glucose by other glycosyl hydrolases including a previously characterized α-glucosidase enzyme (47). Extracellular glycogen breakdown products can also be utilized by other resident microbiota.

Acknowledgements:

This research was supported by a Natural Sciences and Engineering Research Council of Canada Discovery Grant (J.E.H.) and Agriculture and Agri-Food Canada (D.W.A. project no. J-002262). P.B. is supported by a Devolved Scholarship from the University of Saskatchewan. The authors would like to thank Champika Fernando for technical support, Shubham Dutta for guidance with Western blot, and Noreen Rapin and Dr. Tony Ruzzini for providing reagents.

481 **References**

482 1. Hillier SL. 1993. Diagnostic microbiology of bacterial vaginosis. Am J Obstet Gynecol
483 169:455–459.

484 2. Muzny CA, Schwebke JR. 2020. Asymptomatic bacterial vaginosis: To treat or not to treat?
485 Curr Infect Dis Rep 22:32.

486 3. van de Wijgert JHHM, Borgdorff H, Verhelst R, Crucitti T, Francis S, Verstraelen H,
487 Jespers V. 2014. The vaginal microbiota: what have we learned after a decade of molecular
488 characterization? PLoS ONE 9:e105998.

489 4. Vaneechoutte M, Guschin A, Van Simaey L, Gansemans Y, Van Nieuwerburgh F, Cools P.
490 2019. Emended description of *Gardnerella vaginalis* and description of *Gardnerella*
491 *leopoldii* sp. nov., *Gardnerella piotii* sp. nov. and *Gardnerella swidsinskii* sp. nov., with
492 delineation of 13 genomic species within the genus *Gardnerella*. Int J Syst Evol Microbiol
493 69:679–687.

494 5. Hill JE, Albert AYK. 2019. Resolution and cooccurrence patterns of *Gardnerella leopoldii*,
495 *G. swidsinskii*, *G. piotii*, and *G. vaginalis* within the vaginal microbiome. Infect Immun
496 87:e00532-19.

497 6. Khan S, Voordouw MJ, Hill JE. 2019. Competition among *Gardnerella* subgroups from the
498 human vaginal microbiome. Front Cell Infect Microbiol 9:374.

499 7. Adeva-Andany MM, González-Lucán M, Donapetry-García C, Fernández-Fernández C,
500 Ameneiros-Rodríguez E. 2016. Glycogen metabolism in humans. BBA Clin 5:85–100.

501 8. Cruickshank R, Sharman A. 1934. The biology of the vagina in the human subject. BJOG
502 Int J Obstet Gynaecol 41:208–226.

503 9. Nasioudis D, Beghini J, Bongiovanni AM, Giraldo PC, Linhares IM, Witkin SS. 2015. α-
504 amylase in vaginal fluid: association with conditions favorable to dominance of
505 *Lactobacillus*. Reprod Sci 22:1393–1398.

506 10. Mirmonsef P, Hotton AL, Gilbert D, Gioia CJ, Maric D, Hope TJ, Landay AL, Spear GT.
507 2016. Glycogen levels in undiluted genital fluid and their relationship to vaginal pH,
508 estrogen, and progesterone. PloS One 11:e0153553.

509 11. Lombard V, Golaconda Ramulu H, Drula E, Coutinho PM, Henrissat B. 2014. The
510 carbohydrate-active enzymes database (CAZy) in 2013. Nucleic Acids Res 42:D490–D495.

511 12. Spear GT, French AL, Gilbert D, Zariffard MR, Mirmonsef P, Sullivan TH, Spear WW,
512 Landay A, Micci S, Lee B-H, Hamaker BR. 2014. Human α-amylase present in lower-
513 genital-tract mucosal fluid processes glycogen to support vaginal colonization by
514 *Lactobacillus*. J Infect Dis 210:1019–1028.

515 13. Nunn KL, Clair GC, Adkins JN, Engbrecht K, Fillmore T, Forney LJ. 2020. Amylases in
516 the human vagina. mSphere 5:e00943-20.

517 14. Schellenberg JJ, Paramel Jayaprakash T, Withana Gamage N, Patterson MH, Vaneechoutte
518 M, Hill JE. 2016. *Gardnerella vaginalis* subgroups defined by cpn60 sequencing and
519 Sialidase activity in isolates from Canada, Belgium and Kenya. PloS One 11:e0146510.

520 15. Ryan SM, Fitzgerald GF, van Sinderen D. 2006. Screening for and identification of starch-,
521 amylopectin-, and pullulan-degrading activities in Bifidobacterial Strains. Appl Environ
522 Microbiol 72:5289.

523 16. Cockburn D, Koropatkin N. 2015. Product analysis of starch active enzymes by TLC.
524 Bioprotocol 5:1–8.

525 17. Martín-Platero AM, Valdivia E, Maqueda M, Martínez-Bueno M. 2007. Fast, convenient,
526 and economical method for isolating genomic DNA from lactic acid bacteria using a
527 modification of the protein "salting-out" procedure. Anal Biochem 366:102–104.

528 18. Vancuren SJ, Hill JE. 2019. Update on cpnDB: a reference database of chaperonin
529 sequences. Database 2019.

530 19. Hill JE, Penny SL, Crowell KG, Goh SH, Hemmingsen SM. 2004. cpnDB: A chaperonin
531 sequence database. Genome Res 14:1669–1675.

532 20. Kolmogorov M, Yuan J, Lin Y, Pevzner PA. 2019. Assembly of long, error-prone reads
533 using repeat graphs. Nat Biotechnol 37:540–546.

534 21. Aziz RK, Bartels D, Best AA, DeJongh M, Disz T, Edwards RA, Formsma K, Gerdes S,
535 Glass EM, Kubal M, Meyer F, Olsen GJ, Olson R, Osterman AL, Overbeek RA, McNeil
536 LK, Paarmann D, Paczian T, Parrello B, Pusch GD, Reich C, Stevens R, Vassieva O,
537 Vonstein V, Wilke A, Zagnitko O. 2008. The RAST Server: Rapid annotations using
538 subsystems technology. BMC Genomics 9:75.

539 22. Zhang H, Yohe T, Huang L, Entwistle S, Wu P, Yang Z, Busk PK, Xu Y, Yin Y. 2018.
540 dbCAN2: a meta server for automated carbohydrate-active enzyme annotation. Nucleic
541 Acids Res 46:W95–W101.

542 23. Krogh A, Larsson B, von Heijne G, Sonnhammer ELL. 2001. Predicting transmembrane
543 protein topology with a hidden markov model: application to complete genomes11Edited
544 by F. Cohen. J Mol Biol 305:567–580.

545 24. Zhou M, Boekhorst J, Francke C, Siezen RJ. 2008. LocateP: Genome-scale subcellular-
546 location predictor for bacterial proteins. BMC Bioinformatics 9:173.

547 25. Robert X, Gouet P. 2014. Deciphering key features in protein structures with the new
548 ENDscript server. Nucleic Acids Res 42:W320–W324.

549 26. Schlager B, Straessle A, Hafen E. 2012. Use of anionic denaturing detergents to purify
550 insoluble proteins after overexpression. BMC Biotechnol 12:95.

551 27. Kahar UM, Latif NA, Amran SI, Liew KJ, Goh KM. 2022. A bibliometric analysis and
552 review of pullulan-degrading enzymes—past and current trends. Catalysts 12:143.

553 28. Uitdehaag JCM, Mosi R, Kalk KH, van der Veen BA, Dijkhuizen L, Withers SG, Dijkstra
554 BW. 1999. X-ray structures along the reaction pathway of cyclodextrin glycosyltransferase
555 elucidate catalysis in the α-amylase family. Nat Struct Biol 6:432–436.

556 29. Muzny CA, Schwebke JR. 2016. Pathogenesis of bacterial vaginosis: discussion of current
557 hypotheses. J Infect Dis 214:S1–S5.

558 30. Muzny CA, Taylor CM, Swords WE, Tamhane A, Chattopadhyay D, Cerca N, Schwebke
559 JR. 2019. An Updated Conceptual Model on the Pathogenesis of Bacterial Vaginosis. J
560 Infect Dis 220:1399–1405.

561 31. Atassi F, Brassart D, Grob P, Graf F, Servin AL. 2006. *Lactobacillus* strains isolated from
562 the vaginal microbiota of healthy women inhibit *Prevotella bivia* and *Gardnerella vaginalis*
563 in coculture and cell culture. FEMS Immunol Med Microbiol 48:424–432.

564 32. Castro J, Rosca AS, Cools P, Vaneechoutte M, Cerca N. 2020. *Gardnerella vaginalis*
565 enhances *Atopobium vaginae* viability in an in vitro model. Front Cell Infect Microbiol
566 10:83.

567 33. van der Veer C, Hertzberger RY, Bruisten SM, Tytgat HLP, Swanenburg J, de Kat
568 Angelino-Bart A, Schuren F, Molenaar D, Reid G, de Vries H, Kort R. 2019. Comparative
569 genomics of human *Lactobacillus crispatus* isolates reveals genes for glycosylation and
570 glycogen degradation: implications for in vivo dominance of the vaginal microbiota.
571 Microbiome 7:49.

572 34. Woolston BM, Jenkins DJ, Hood-Pishchany MI, Nahoum SR, Balskus EP. 2021.
573 Characterization of vaginal microbial enzymes identifies amylopullulanases that support
574 growth of *Lactobacillus crispatus* on glycogen. preprint. Biochemistry.

575 35. Edmunds PN. 1962. The biochemical, serological and haemagglutinating reactions of
576 *Haemophilus vaginalis*. J Pathol Bacteriol 83:411–422.

577 36. Piot P, Van Dyck E, Totten PA, Holmes KK. 1982. Identification of *Gardnerella*
578 (*Haemophilus*) *vaginalis*. J Clin Microbiol 15:19–24.

579 37. Dunkelberg WE, McVeigh I. 1969. Growth requirements of *Haemophilus vaginalis*.
580 Antonie Van Leeuwenhoek 35:129–145.

581 38. Huffman RD, Nawrocki LD, Wilson WA, Brittingham A. 2015. Digestion of glycogen by
582 α-glucosidase released by *Trichomonas vaginalis*. Exp Parasitol 159:151–159.

583 39. Hii SL, Tan JS, Ling TC, Ariff AB. 2012. Pullulanase: role in starch hydrolysis and
584 potential industrial applications. Enzyme Res 2012:1–14.

585 40. Boraston AB, Healey M, Klassen J, Ficko-Blean E, van Bueren AL, Law V. 2006. A
586 structural and functional analysis of α-glucan recognition by family 25 and 26
587 carbohydrate-binding modules reveals a conserved mode of starch recognition. J Biol Chem
588 281:587–598.

589 41. Cantarel BL, Coutinho PM, Rancurel C, Bernard T, Lombard V, Henrissat B. 2009. The
590 Carbohydrate-Active EnZymes database (CAZy): an expert resource for glycogenomics.
591 Nucleic Acids Res 37:D233–D238.

592 42. Cockburn DW, Suh C, Medina KP, Duvall RM, Wawrzak Z, Henrissat B, Koropatkin NM.
593 2018. Novel carbohydrate binding modules in the surface anchored α-amylase of
594 *Eubacterium rectale* provide a molecular rationale for the range of starches used by this
595 organism in the human gut. Mol Microbiol 107:249–264.

596 43. Kim S-Y, Kim H, Kim Y-J, Jung D-H, Seo D-H, Jung J-H, Park C-S. 2021. Enzymatic
597 analysis of truncation mutants of a type II pullulanase from *Bifidobacterium adolescentis*
598 P2P3, a resistant starch-degrading gut bacterium. Int J Biol Macromol 193:1340–1349.

599 44. Ghosh S, O'Connor TJ. 2017. Beyond paralogs: the multiple layers of redundancy in
600 bacterial pathogenesis. Front Cell Infect Microbiol 7:467.

601 45. Siegel SD, Reardon ME, Ton-That H. 2016. Anchoring of LPXTG-like proteins to the
602 gram-positive cell wall envelope, p. 159–175. *In* Bagnoli, F, Rappuoli, R (eds.), Protein and
603 Sugar Export and Assembly in Gram-positive Bacteria. Springer International Publishing,
604 Cham.

605 46. Agarwal K, Lewis AL. 2021. Vaginal sialoglycan foraging by *Gardnerella vaginalis* :
606 mucus barriers as a meal for unwelcome guests? Glycobiology 31:667–680.

607 47. Bhandari P, Tingley JP, Palmer DRJ, Abbott DW, Hill JE. 2021. Characterization of an α-
608 glucosidase enzyme conserved in *Gardnerella* spp. isolated from the human vaginal
609 microbiome. J Bacteriol 203.

610 48. Boos W, Shuman H. 1998. Maltose/maltodextrin system of *Escherichia coli*: transport,
611 metabolism, and regulation. Microbiol Mol Biol Rev 62:204–229.

612

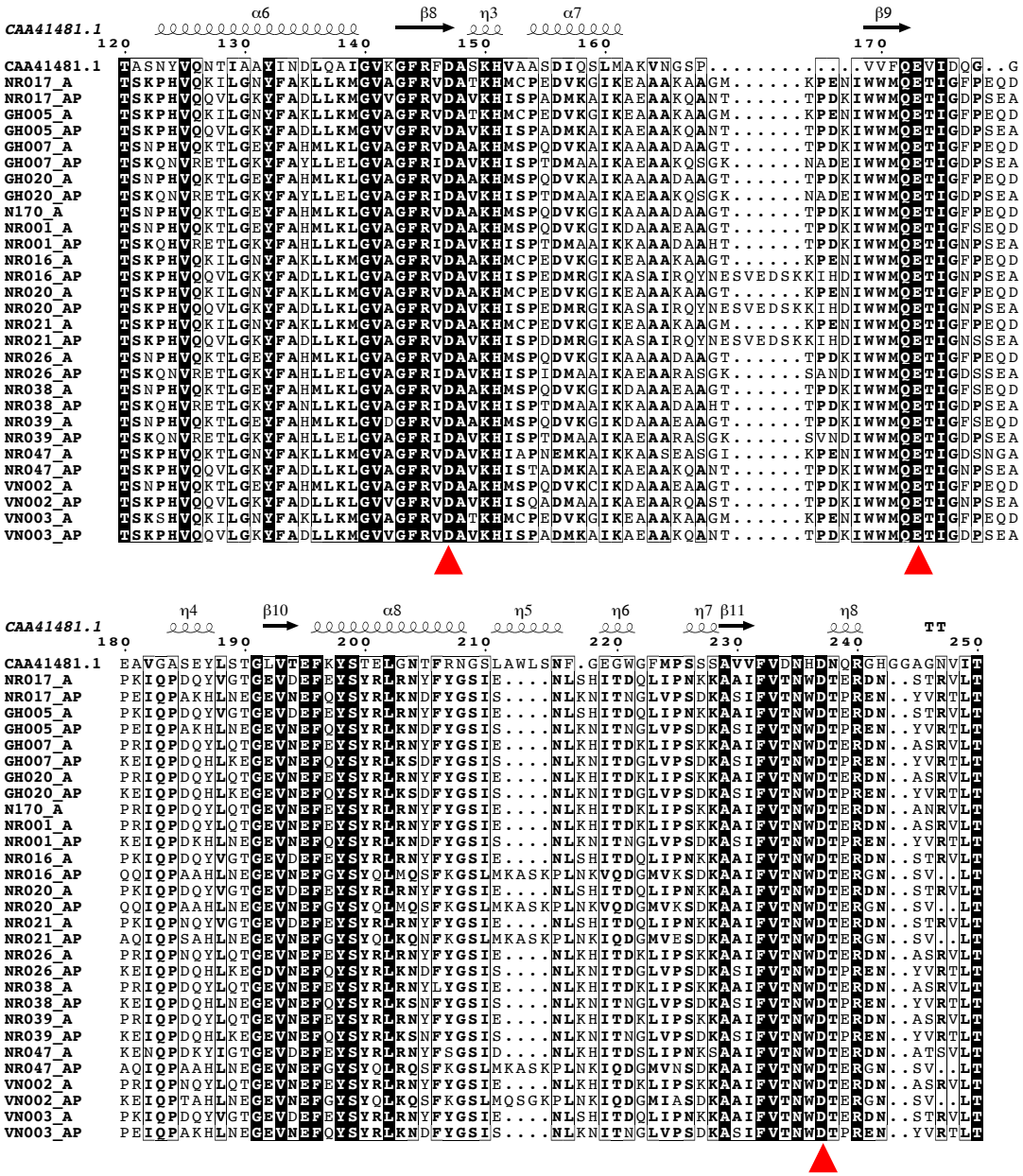

Supplementary Figure 1: Sequence alignment of all GH13_32 domains from 15 *Gardnerella* isolates with GH13_32 domain of functionally characterized α-amylase from *P. haloplanktis* A23 (CAA41481.1). An alignment including amino acids from 120 to 250 positions only is shown. Conserved catalytic residues are indicated with red triangles and invariant sequences are highlighted in dark background.

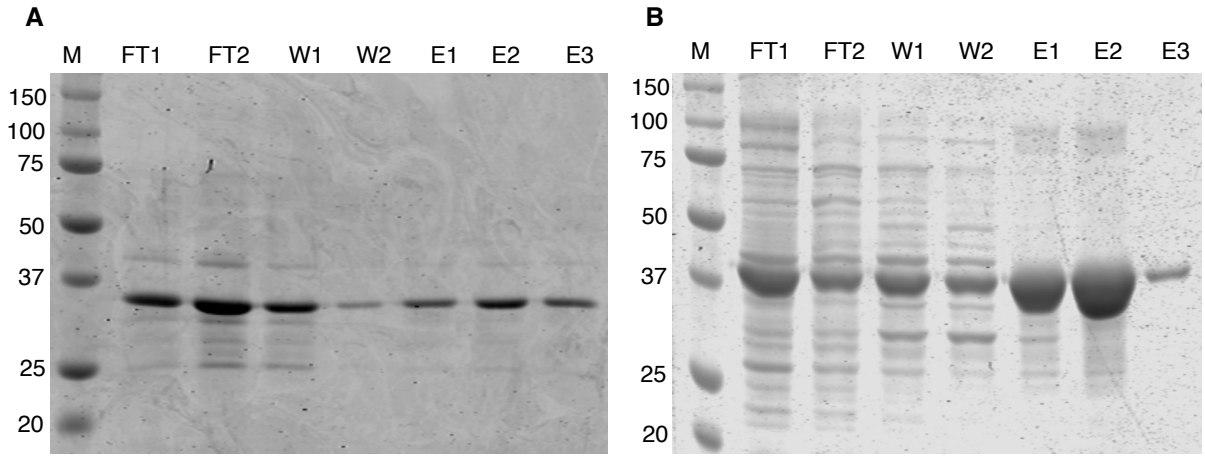

Supplementary Figure 2: Ni-NTA purification of 6His-tagged amylase (A) and pullulanase (B) domain proteins. M: molecular weight marker, FT1 &FT2: flow through fractions, W1&W2: wash fractions, E1-E3: elution fractions.

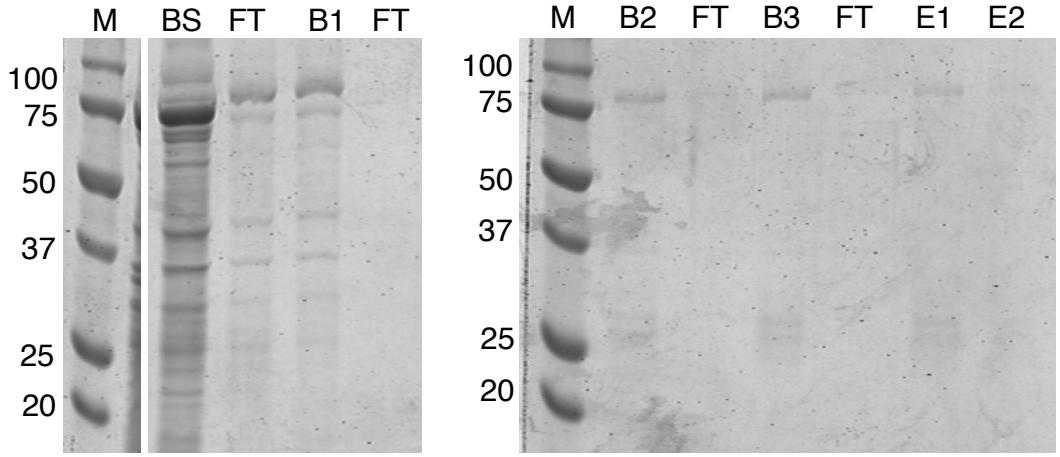

Supplementary Figure 3: Analysis of fractions obtained during protein purification using glutathione beads. M: molecular weight markers, BS: mixture of glutathione beads and solubilized protein, FT: flowthroughs, B1-B3: Protein bound glutathione beads obtained after first, second and third wash, E1-E2: elution fractions

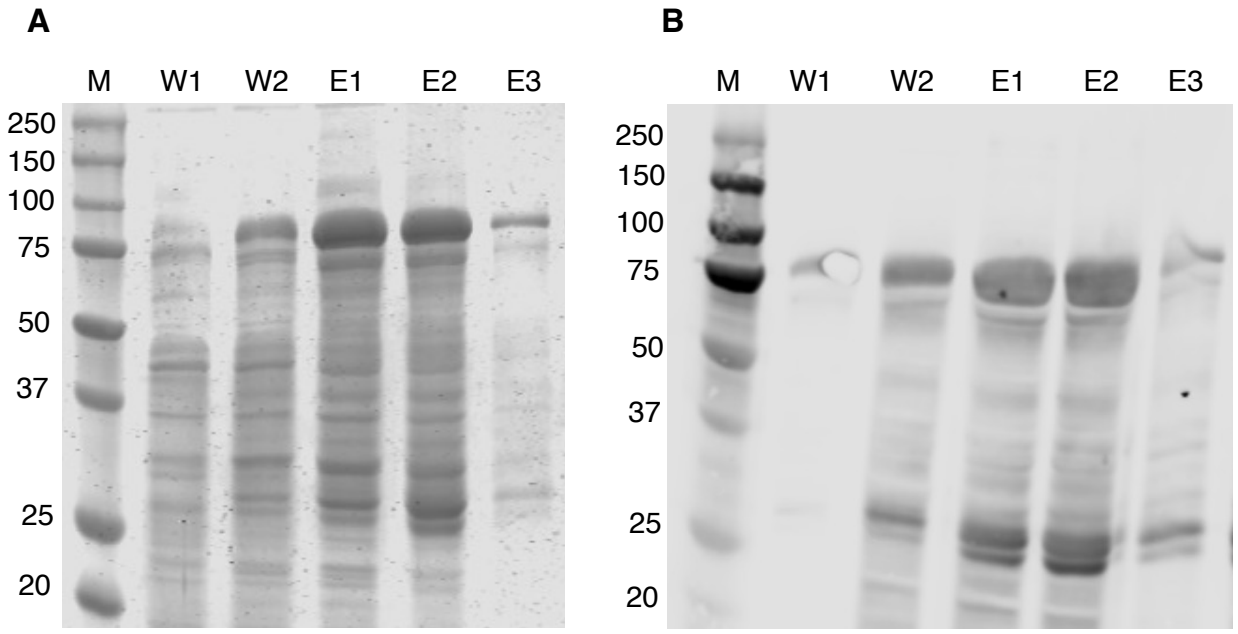

Supplementary Figure 4: SDS-PAGE (A) and Western blot (B) analysis of fractions obtained during recombinant α-amylase protein purification using Nickel affinity chromatography (A). Immunoblot membrane was first incubated with primary antibody (Anti-6x His tag monoclonal antibody, 1:2,000 dilutions) followed by washing and further incubation with secondary antibody conjugates (Alexa fluor 680 goat anti-mouse IgG, 1: 20,000 dilutions). Finally, membrane was scanned at 700 nm using Li-COR scanner after secondary antibody wash. M- molecular weight markers, W1 & W2: wash fractions, E1-E3: elution fractions.

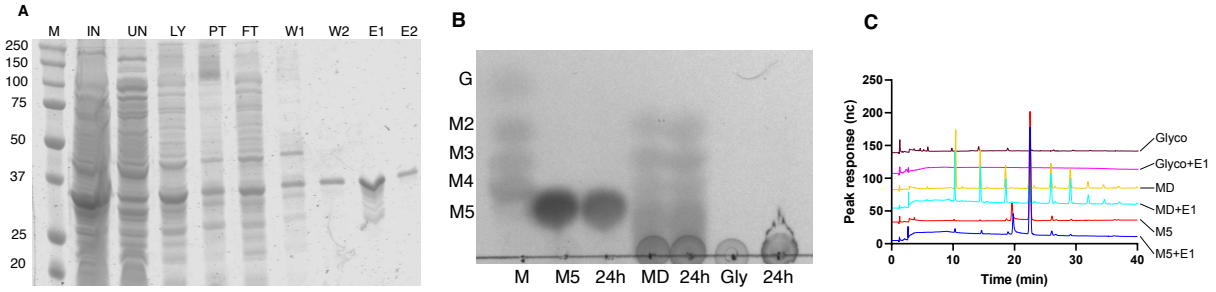

Supplementary Figure 5: (A) Expression and Ni-NTA purification of GST-His fusion tag. M: molecular weight markers, IN: IPTG induced culture, UN: uninduced culture, LY: lysate, PT: pellet, FT: flowthrough, W1 and W2: wash fractions, E1 and E2: elution fractions. Identification of products obtained from purified GST-His tag with maltopentose (M5), maltodextrin (MD) and Glycogen (Gly) using TLC (B) and HPAEC-PAD (C). M: sugar standards: G: glucose, M2: maltose, M3: maltotriose, M4: maltotetraose.

Supplementary Table 1: Primers used in this study. Restriction endonuclease recognition sites are underlined.

Primer ID	Sequence (5'-3')	RE sites
JH0729	CGC CAG GGT TTT CCC AGT CAC GAC GAI III GCI GGI GAY GGI ACI ACI AC	
JH0730	AGC GGA TAA CAA TTT CAC ACA GGA YKI YKI TCI CCR AAI CCI GGI GCY TT	
JH0810	AAT GGA TCC GAG TGC ACT AAA ACT TAC GGT CAT	*Bam*HI
JH0811	ATG GTA CCG TAC CCT GAA TAA ATG TTT GGG	*Kpn*I
JH0812	CAG GGA TCC ACT AAG AAT GGA AGC AAG CCA ACT GGT	*Bam*HI
JH0813	ATG GTA CCA TTC TTA TTG CCG TTC TTG CTT CGT AAG	*Kpn*I
JH0857	GAT CAA TTG CTT CCA CAA AAT CCA CTG	*Mfe*I
JH0858	ACT AAG CTT TTA CGA AGT CGA TCC GAA	*Hind*III